EUKARYOTIC CELL, Jan. 2007, p. 95–109 Vol. 6, No. 1
1535-9778/07/$08.00+0 doi:10.1128/EC.00306-06

Radial Mass Density, Charge, and Epitope Distribution in the *Cryptococcus neoformans* Capsule▽

Michelle E. Maxson,[1] Ekaterina Dadachova,[1,2] Arturo Casadevall,[1,3]†* and Oscar Zaragoza[1]†*

Departments of Microbiology and Immunology,[1] Medicine,[3] and Nuclear Medicine,[2] Albert Einstein College of Medicine, 1300 Morris Park Avenue, Bronx, New York 10461

Received 26 September 2006/Accepted 10 November 2006

Exposure of *Cryptococcus neoformans* cells to gamma radiation results in a gradual release of capsular polysaccharide, in a dose-dependent manner. This method allows the systematic exploration of different capsular regions. Using this methodology, capsule density was determined to change according to the radial distribution of glucuronoxylomannan and total polysaccharide, becoming denser at the inner regions of the capsule. Scanning electron microscopy of cells following gamma radiation treatment confirmed this finding. The zeta potential of the capsule also increased as the capsule size decreased. However, neither charge nor density differences were correlated with any change in sugar composition (xylose, mannose, and glucuronic acid) in the different capsular regions, since the proportions of these sugars remained constant throughout the capsule. Analysis of the capsular antigenic properties by monoclonal antibody binding and Scatchard analysis revealed fluctuations in the binding affinity within the capsule but not in the number of antibody binding sites, suggesting that the spatial organization of high- and low-affinity epitopes within the capsule changed according to radial position. Finally, evidence is presented that the structure of the capsule changes with capsule age, since the capsule of older cells became more resistant to gamma radiation-induced ablation. In summary, the capsule of *C. neoformans* is heterogeneous in its spatial distribution and changes with age. Furthermore, our results suggest several mechanisms by which the capsule may protect the fungal cell against exogenous environmental factors.

Capsules are a common feature among microorganisms, especially pathogenic bacteria such as *Bacillus anthracis*, *Streptococcus pneumoniae*, and *Neisseria meningitidis*. Microbial capsules can confer particular characteristics, such as protection against stress conditions (64), and are prominent virulence factors. In contrast to the situation in bacteria, extracellular capsules are rare in fungi. The only encapsulated pathogenic fungus is the basidiomycetous yeast *Cryptococcus neoformans*. This fungus is commonly found in the environment, inhabiting various niches such as pigeon droppings, trees, and water (reviewed in reference 8). The pathogenesis of *C. neoformans* has been well studied. The yeast is commonly acquired by the host via inhalation. The infection is asymptomatic in immunocompetent hosts. However, in cases of immune suppression, pulmonary infection can be followed by extrapulmonary dissemination of the yeast into other organs, such as spleen, liver, and brain. Untreated cryptococcal meningitis is invariably fatal.

The polysaccharide capsule of *C. neoformans* is considered the main virulence factor of this pathogen (37). Acapsular *C. neoformans* strains manifest greatly reduced virulence (10, 31), and mutants that produce a larger capsule are hypervirulent (19). The capsule of this yeast is believed to function in protection from desiccation, radiation, and predation by phagocytic organisms (reviewed in reference 9). During pathogen-host interactions, the *C. neoformans* capsular polysaccharide is abundantly released into tissues (24) and has been associated with a myriad of deleterious immunological effects including antibody (Ab) unresponsiveness (27, 47), inhibition of leukocyte migration (18), complement depletion (34), deregulation of cytokine production (53, 62, 63), and interference with antigen presentation (53). In addition, the capsular polysaccharide inhibits phagocytosis of the yeast by phagocytic cells (26, 70).

While the role of the *C. neoformans* capsule in virulence has been extensively studied, relatively little is known about the organization of this enigmatic structure. The capsule is composed of three basic elements, glucuronoxylomannan (GXM), representing 90 to 95% of the polysaccharide; galactoxylomannan (GalXM), 5%; and mannoproteins, less than 1% (52; reviewed in references 5, 17, and 38). However, a recent study suggests that GalXM could be the major component in molar composition (40). All capsule-related structural studies have been based on analysis of GXM from capsular polysaccharide shed by *C. neoformans* (12). Shed GXM is known to be a high-molecular-mass polysaccharide (1.7 to 7.3 MDa, depending on serotype) with a complex structure (2, 3, 40, 58, 60). These studies also demonstrate that GXM contains six basic repeats of mannose chains that can be replaced in many combinations with xylose or glucuronic acid and organized fibers. The mannose backbone of the GXM can be O acetylated, and this substitution is known to confer immunogenic characteristics (28, 39, 45). Although much work has focused on capsular exopolysaccharide, little is known about the nature of the poly-

* Corresponding author. Present address for Oscar Zaragoza: Servicio de Micología, Centro Nacional de Microbiología, Instituto de Salud Carlos III, Ctra. Majadahonda-Pozuelo Km 2, Majadahonda, Madrid 28220, Spain. Phone: 34918223661. Fax: 34915097034. E-mail: ozaragoza@isciii.es. Mailing address for Arturo Casadevall: Departments of Microbiology and Immunology and Medicine, Albert Einstein College of Medicine, 1300 Morris Part Avenue, Bronx, New York 10461. Phone: (718) 430-3665. Fax: (718) 430-8701. E-mail: casadeva@aecom.yu.edu.

† Arturo Casadevall and Oscar Zaragoza share senior authorship of this paper.

▽ Published ahead of print on 17 November 2006.

saccharide retained on the *C. neoformans* cell. The capsule can be noncovalently attached to the cell body via the alpha-1,3-glucan of the cell wall (51). Recent findings have shown that the capsule is a dynamic structure, subjected to changes according to the environment (see review in reference 41). One peculiar feature of the *C. neoformans* capsule is that it changes in size according to environmental conditions (25, 61, 66, 68) and is dramatically enlarged upon interaction with mammalian hosts (4, 14, 21, 33, 55). Although there are several models for capsule growth (50), recent evidence supports the hypothesis that the capsule grows by apical enlargement, which may involve the addition of new fibers that attach to the existing polysaccharide through noncovalent bonds (40, 71). The spatial distribution of the capsular material is not equal throughout the capsule. Electron microscopy images and studies of penetration of fluorescently labeled dextrans suggest that the capsule is denser in the regions close to the cell wall (23, 50).

In the early 1970s, it was reported that extremely high doses of gamma radiation greatly reduced the size of the *C. neoformans* capsule (16), but this phenomenon was largely forgotten until recently, when it was rediscovered and examined in detail (6). Doses of gamma radiation that are thousands of times lower than those previously described (16) release capsular polysaccharide very efficiently, by a presumed mechanism involving the creation of free radicals from solution (6). This reaction occurs without affecting the viability of *C. neoformans*, which is gamma radiation resistant (6). In the present study, gamma radiation is utilized to investigate the structure of the *C. neoformans* capsule that is retained on the cell. Our results demonstrate quantitative and qualitative radial differences in polysaccharide composition, highlighting unsuspected complexity.

MATERIALS AND METHODS

Strains and growth conditions. *C. neoformans* strain H99 (serotype A) was used (49). This strain was selected because it is representative of the most prevalent pathogenic serotype, is a standard *C. neoformans* strain, and provides a population with homogenous capsule and cell size during both log-phase growth and capsule induction (68). In some experiments, the acapsular *cap67* mutant was used (10). The cells were routinely grown in Sabouraud dextrose medium (Sab), at 30°C with minimal shaking (150 rpm). To induce capsule growth, cells were first grown overnight as described above, collected by centrifugation, washed three times in phosphate-buffered saline (PBS), and counted using a hemocytometer. Then, cells were used to inoculate 10 ml of capsule-inducing medium (10% Sab in 50 mM MOPS [morpholinepropanesulfonic acid; pH 7.4]) (66) to a final concentration of 1×10^7 cells/ml. Capsule induction was performed in 100-mm petri plates, incubated overnight at 37°C without shaking. In some experiments, capsule enlargement was induced in 500 ml of inducing medium with moderate shaking (150 rpm). Alternatively, to study the effect of cell age on capsule properties, cells were grown and induced as described above, but in addition, cells were induced at 37°C for 7 or 14 days. In some cases, prior to inoculation into capsule-inducing medium, the cell wall was labeled first in a solution of 4-mg/ml EZ-Link sulfo-NHS-LC-biotin [sulfosuccinimidyl-6-(biotinamido)hexanoate] in PBS (Pierce, IL) for 1 h at room temperature at a cell density of 5×10^7 cells/ml, extensively washed with PBS, and then placed in the capsule induction medium for the period of time indicated in the text. Biotinylated cells were detected using streptavidin-fluorescein isothiocyanate (FITC; 20 μg/ml; Biosource, Camarillo, CA).

Gamma radiation treatment. Yeast cells with enlarged capsule were exposed to various amounts of gamma radiation from radioisotope ^{137}Cs, to remove layers of the polysaccharide capsule by free radical attack. Briefly, capsule-induced cells were washed three times in PBS to remove shed capsular polysaccharides and suspended in PBS or H_2O, and 5×10^7 cells were radiated using the Shepherd Mark I irradiator (JL Shepherd and Associates, San Fernando, CA) at the dose rate of 1,388 rads/min. For all experiments, cells were irradiated for 0, 5, 10, 20, 30, or 40 min. Irradiated cells were collected by centrifugation. The supernatants containing shaved capsular polysaccharide were saved for analysis (see below). Radiated cells were washed three times in PBS and saved for analysis (see below). In a similar experiment, the cells were irradiated for 20 min and centrifuged. The supernatant was kept at 4°C (0- to 20-min sample); meanwhile the cells washed with H_2O were resuspended in fresh H_2O and irradiated for another 20 min. After this irradiation, cells were centrifuged and the supernatant collected (20- to 40-min sample).

India ink staining and capsule size measurement. The *C. neoformans* capsule was visualized after suspension of the cells in India ink or by immunofluorescence using sulfo-NHS-LC-biotin and streptavidin-FITC labeling of the cell wall (see above) and 18B7 (5 μg/ml) (46)/goat anti-mouse immunoglobulin G1 (IgG1)–tetramethyl rhodamine isothiocyanate (TRITC; 5 μg/ml) labeling of the capsular edge. Samples were observed using an Olympus AX70 microscope, QCapture Suite V2.46 software for Windows, and Adobe Photoshop 7.0 for Macintosh. To calculate capsule relative size, the diameters of the whole cell, including capsule (D_{wc}), and cell body, limited by the cell wall (D_{cb}), were measured using Adobe Photoshop 7.0 for Macintosh. The size of the capsule relative to that of the whole cell was defined, as a percentage, as $[(D_{wc} - D_{cb})/D_{wc}] \times 100$. Twenty cells were measured for each determination, and the average and standard deviation were calculated. In some cases, percent capsule volume after gamma irradiation (V_p) was also calculated from the volume (in μl) of cell packing in hematocrit capillary tubes (36). Hematocrit volume per cell (HVPC) was calculated as V_p/number of cells. Percent capsule volume after gamma irradiation was defined as $(HVPC_{postirradiation}/HVPC_{nonirradiated}) \times 100$. Alternatively, whole-cell volume (V_{wc}) was calculated from immunofluorescence images, defined as $(4/3)\ \pi\ (D_{wc}/2)^3$. Capsule volume was defined as the difference between the volume of the cell with capsule and the volume of the cell without capsule. Percent capsule volume after gamma irradiation was calculated as $(V_{wc\ postirradiation}/V_{wc\ nonirradiated}) \times 100$.

GXM measurement. Soluble GXM was measured by capture enzyme-linked immunosorbent assay (ELISA) as described in reference 7. Briefly, 96-well plates were coated with goat anti-mouse IgM (1 μg/ml; Southern Biotechnology Associates, Birmingham, AL) followed by capture antibody 2D10 (2 μg/ml) (46). Samples were added and detected using primary monoclonal antibody (MAb) 18B7 (2 μg/ml) (46) and secondary antibody goat anti-mouse IgG1 conjugated to alkaline phosphatase (1 μg/ml; Southern Biotechnology Associates, Birmingham, AL). One milligram per milliliter *p*-nitrophenyl phosphate dissolved in substrate buffer (1 mM $MgCl_2 \cdot 6H_2O$; 50 mM Na_2CO_3) was used for development, and absorbance was measured at 405 nm, using a microplate reader after incubation at room temperature for approximately 20 min.

Total polysaccharide measurements. The concentration of total polysaccharide was determined in each of the gamma-irradiated cryptococcal cell supernatants, using the phenol-sulfuric acid colorimetric technique (20).

Complement deposition on the *C. neoformans* capsule. Complement (complement protein 3 [C3]) deposition on the cryptococcal capsule was performed as described in reference 70. Briefly, blood from C57BL/6J female mice (6 to 8 weeks old; National Cancer Institute) was obtained from the retro-orbital cavity, and serum was obtained after centrifugation. Cryptococcal cells (2×10^7) were suspended in 700 μl freshly obtained serum and incubated at 37°C for 1 h. Cells were extensively washed and suspended in PBS. Samples containing 3×10^6 cells were gamma irradiated for 0, 5, 10, 20, 30, or 40 min, as described above. C3 was then detected using an FITC-conjugated goat anti-mouse C3 antibody (4 μg/ml; Cappel, ICN, Aurora, OH). To detect the capsular edge, MAb 18B7 (10 μg/ml) was added and detected using a TRITC-conjugated goat anti-mouse IgG1 antibody (10 μg/ml; Southern Biotechnology Associates, Inc., Birmingham, AL). The cells were observed under fluorescent filters with the Olympus AX70 microscope, QCapture Suite V2.46 software for Windows, and Adobe Photoshop 7.0 for Macintosh.

MAb 18B7 protection of the *C. neoformans* capsule release. A suspension of 5×10^6 cryptococcal cells in 750 μl was incubated with either 0, 10, 50, 100, or 500 μg/ml of MAb 18B7 for 1 h. Cells were extensively washed and suspended in PBS. Samples were then exposed to gamma radiation for 20 min. MAb 18B7 that remained on the capsule was then detected using an FITC-conjugated goat anti-mouse IgG1 antibody (5 μg/ml). Cells were observed under fluorescent filters with the Olympus AX70 microscope, QCapture Suite V2.46 software for Windows, and Adobe Photoshop 7.0 for Macintosh.

Scanning electron microscopy (SEM). Approximately 5×10^7 irradiated yeast cells were washed in PBS three times and suspended in fixing solution (2% *p*-formaldehyde, 2.5% glutaraldehyde, 0.1 M sodium cacodylate). Cells were then serially dehydrated with ethanol, coated with gold palladium, and visualized using a JEOL (Tokyo, Japan) JAM 6400 microscope.

Measurement of zeta potential. Approximately 5×10^7 yeast cells were washed and suspended in 1 mM KCl. Zeta potential measurements of the capsule surface

were made using the ZetaPlus zeta potential analyzer (Brookhaven Instruments, Holtsville, NY).

Glycosyl composition analysis of supernatants from gamma-irradiated cryptococcal cells. Approximately 1×10^{10} cells with enlarged capsule were washed, suspended in distilled water, and gamma irradiated for 0 to 20 min or 20 to 40 min as described above. Supernatant samples were lyophilized and analyzed for glycosyl composition at the Complex Carbohydrate Research Center at the University of Georgia (Atlanta) (65). Analysis was performed on 0.2 mg of the lyophilized samples by combined gas chromatography-mass spectrometry of the per-*O*-trimethylsilyl derivatives of the monosaccharide methyl glycosides produced from the sample by acidic methanolysis.

Elemental analysis of material released from gamma-irradiated cryptococcal cells. Supernatants were prepared as described for the sugar composition analysis. Lyophilized samples were then submitted to Quantitative Technologies, Inc. (Whitehouse, NJ), for quantitative elemental analysis. C, H, O, and N were measured with a PE 2400 CHN analyzer fitted with an oxygen accessory kit. Samples were converted into gases by combustion, and product gases were separated by gas chromatography. The elemental percentages were detected by thermal conductivity.

Scatchard analysis. Approximately 2×10^6 gamma-irradiated cells were incubated for 1 h at 37°C with 0.11, 0.22, 0.44, 0.66, or 0.88 nM ^{188}Re-18B7. The radioactivity of the treated samples was counted in a gamma counter, the cells were collected by centrifugation, and the radioactivity of the pellets was counted in a gamma counter. Scatchard analysis (56), to compute the binding constant and the number of binding sites per cell for 18B7, was performed as described previously (32).

Confocal microscopy and 3D reconstruction. Immunofluorescence was performed after labeling the capsule of 1×10^6 induced cryptococcal cells with the following: calcofluor (50 μg/ml), FITC- or TRITC-conjugated 18B7 (3 μg/ml), and 12A1 or 13F1 (IgM antibodies [46], 10 μg/ml) followed by goat anti-mouse IgM conjugated to FITC or TRITC (5 μg/ml). Emissions from 410 to 480 nm (calcofluor), 495 to 535 nm (FITC), and 566 to 648 nm (TRITC) were visualized using a Leica AOBS laser scanning confocal microscope. To obtain three-dimensional (3D) images, a *z* series of each cell was obtained in 0.25-μm slices, and 3D images were processed with ImageJ (NIH) and Voxx (Indiana University) software.

RESULTS

Kinetics of capsule decrease after gamma radiation treatment. Gamma radiation exposure of *C. neoformans* cells results in capsular polysaccharide release (6). This effect provided a means to study the radial composition of the capsule in a graded fashion. The capsule of *C. neoformans* strain H99 is normally 1 to 2 μm in diameter, but the diameter increases to 5 to 8 μm under capsule induction conditions (68). Cryptococcal cells with the enlarged capsule were used for two reasons. First, a larger capsule size made it easier to observe different capsular regions and improved the visible resolution of the capsule so that changes after gamma radiation treatment were easier to see. Second, capsule enlargement represents one of the first morphological changes that occur after host infection.

Capsule size gradually decreased as a function of irradiation time without affecting the size of the cell body, delimited by the cell wall (Fig. 1A). Therefore, it is possible to expose several internal regions of the capsule by this method. The amount of radiation used to induce capsule release has no significant effect on cell viability (6). We then measured the size of the capsule relative to the size of the cell body. After each irradiation period, there was a significant reduction in the relative size of the capsule (Fig. 1B, $P < 0.002$ in all the comparisons). Around 70% of the capsule volume (data not shown) was released after 20 min of irradiation, and longer irradiation times (30 and 40 min) exposed inner regions that remain very close to the cell wall (about 1 μm in distance). Subsequent immunofluorescence analysis showed that after 40 min of irradiation, some capsular polysaccharide still remained, as evidenced by MAb 18B7 binding (see below). However, using this method, several arbitrary layers of the capsule were exposed. Exposure of these layers, which differ in their distances

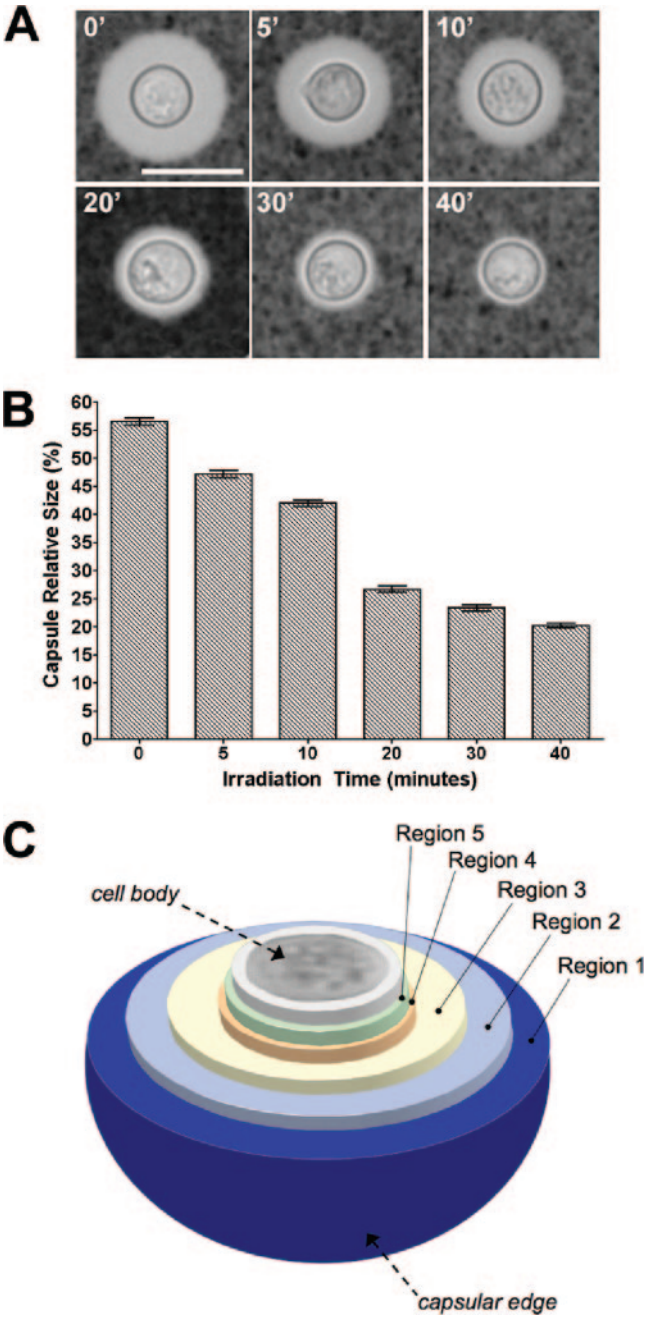

FIG. 1. Kinetics of capsule decrease after gamma radiation treatment. (A) Cells from *C. neoformans* strain H99 with induced, large capsules were exposed to gamma radiation for 0, 5, 10, 20, 30, or 40 min; capsule size was observed by India ink staining of suspended cells. A representative cell from each time point was chosen to illustrate the effect of gamma radiation on capsule size. Bar, 10 μm. (B) Capsule relative size from at least 20 cells was measured as indicated in Materials and Methods. The average and the standard deviation of the relative size of the capsule are plotted. (C) Schematic showing the capsular regions of *C. neoformans* strain H99 exposed after gamma irradiation.

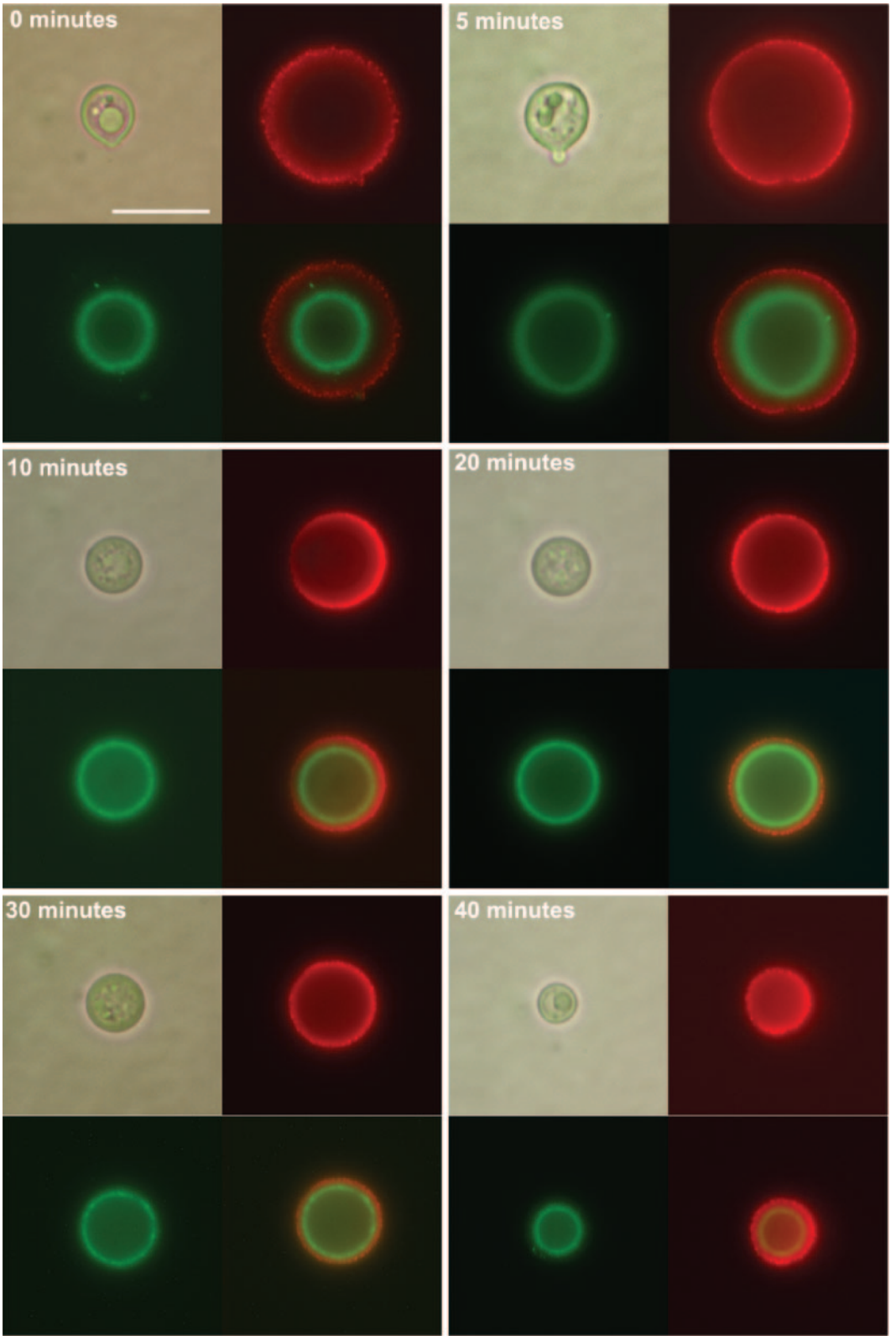

FIG. 2. Bound complement is unaffected by gamma radiation-induced changes in capsule size. Cryptococcal cells with induced capsule were incubated in mouse serum to allow complement deposition on the capsule, which localizes and covalently binds to the inner capsule. Cells were then irradiated for 0, 5, 10, 20, 30, or 40 min, and an immunofluorescence assay was performed to detect complement localization (green fluorescence, FITC). To detect capsule edge, MAb 18B7 was added after the serum incubation and then detected with goat anti-mouse IgG-TRITC. For each time point, upper left panel, light microscopy; upper right panel, rhodamine; lower left panel, FITC; lower right panel, merge of the two fluorescences. Bar, 5 μm.

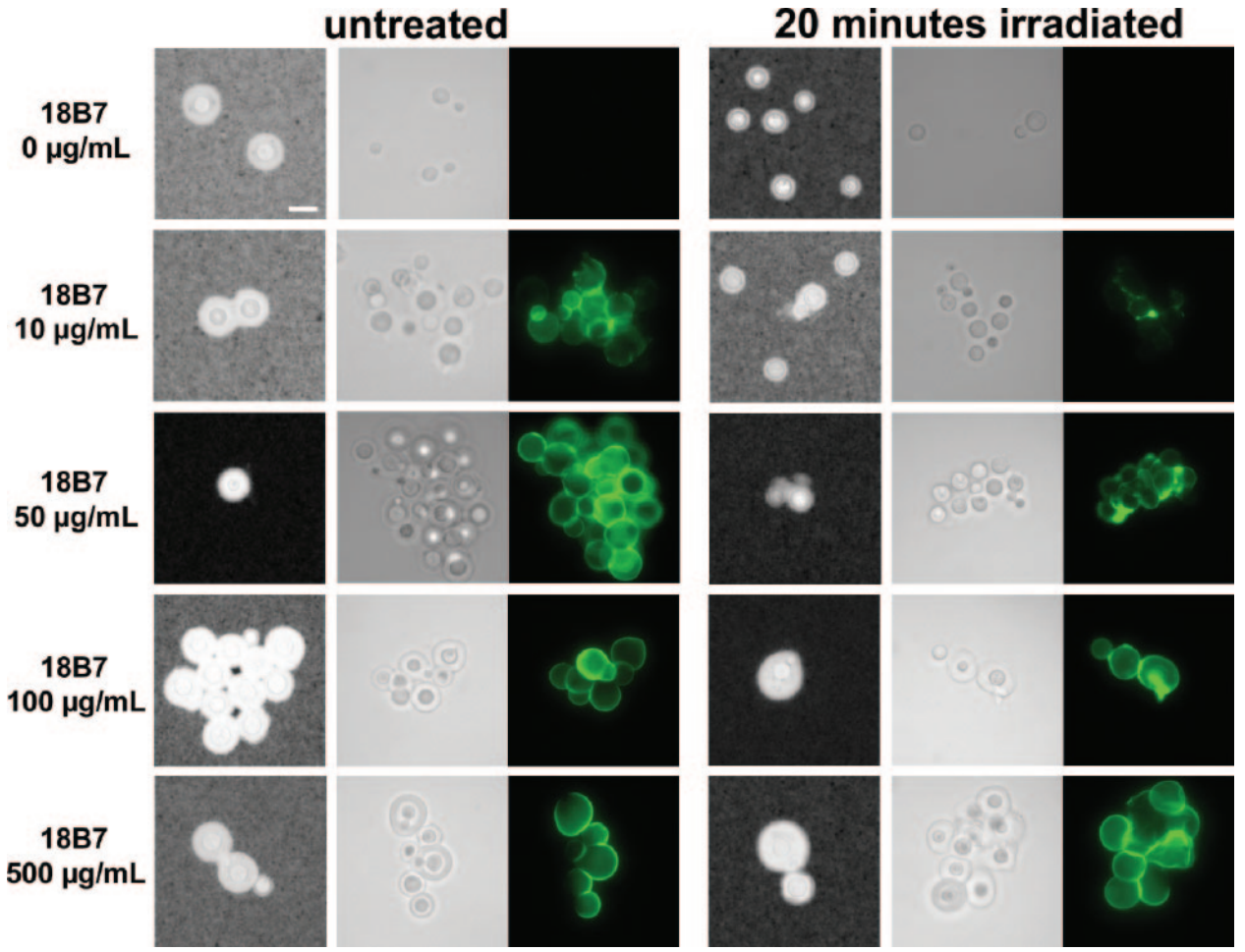

FIG. 3. Gamma radiation of MAb-coated *C. neoformans* cells. Cryptococcal cells with induced capsule were incubated with different concentrations of MAb 18B7. Cells were then irradiated for 20 min and compared to untreated cells. An immunofluorescence assay to detect 18B7 was performed using a goat anti-mouse IgG1-FITC Ab. The cells were suspended in parallel in India ink suspension to visualize the capsule. For each irradiation time: left column, cells suspended in India ink; middle column, light microscopy; right column, 18B7 localization, same field as the middle column. Note how cells present some aggregation, due to the "sticky" properties of Abs. Bar, 5 μm.

from the cell wall, was dependent on the dose of gamma radiation (Fig. 1C).

In interpreting our results, we considered the possibility that the observed decrease in capsule size was the result of an inner collapse mediated by gamma radiation and not the release of the polysaccharide from the capsule exterior. To assess the mode by which gamma radiation released the cryptococcal capsule, the inner capsule was labeled with complement, by incubating the cells in serum, and then the cells were exposed to gamma radiation. Complement (C3) binds to the polysaccharide capsule in the inner part of the capsule, in an interaction that is mediated by the formation of a covalent bond linkage and can be easily observed by fluorescence (70, 71). We observed that when the cells were first placed in serum followed by irradiation, the signal produced by C3 was unaffected, remaining at a location close to the cell wall (Fig. 2). Alternatively, we coated cells with various amounts of MAb 18B7, followed by exposure to 20 min of gamma radiation. MAb 18B7 is known to bind to the outer regions of the cryptococcal capsule (70, 71). Immunofluorescence showed that at low antibody concentrations (10 μg/ml), irradiation resulted in decreased capsule size as well as release of bound MAb 18B7 (Fig. 3). It is noteworthy that the binding of the Ab at these concentrations to the capsule did not change the size of this structure, indicating that only gamma radiation was responsible for capsule size changes in our conditions. We did not use higher concentrations because they have been reported to deform the capsule (67). Therefore, exposure to gamma radiation results in a gradual release of the capsule which occurs at the capsule exterior, without affecting inner capsular regions.

During these experiments, we also observed that MAb 18B7-coated cells were more resistant to capsule shedding by gamma radiation, in a concentration-dependent manner (Fig. 3). The binding of 18B7 in antibody concentrations above 100 μg/ml completely prevented the release of the capsule as measured by capsule size after India ink staining (Fig. 3; see 20-min irradiation), which was confirmed by measurement of capsule relative size by India ink and by capture ELISA to detect GXM in the supernatants of gamma-irradiated cells (data not shown).

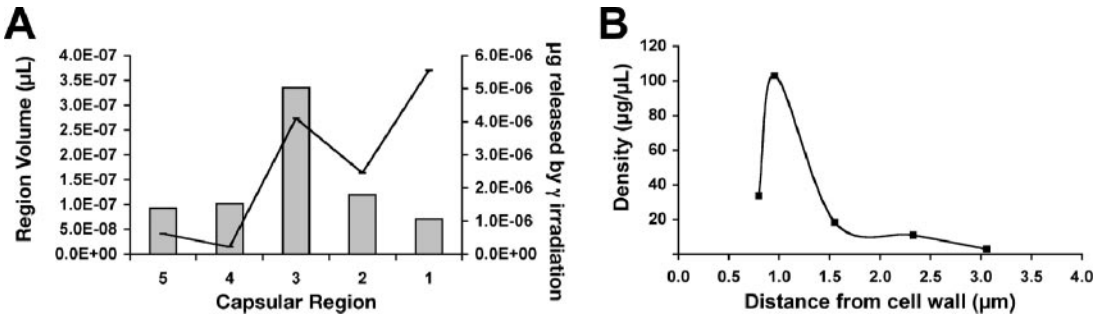

FIG. 4. Polysaccharide density of the capsular layers. (A) After gamma irradiation for 0, 5, 10, 20, 30, or 40 min, we calculated the total amount of GXM (gray bars) contained in each layer, per cell (right axis), and compared this to the layer volume per cell (black line and left axis). See Fig. 1C for the spatial distribution of layers. (B) Using the average amount of GXM per cell (A) and the average volume per layer (A), the average density of total GXM was calculated within the capsule regions. The experiment was duplicated with similar results, and the results of one representative experiment are presented.

Polysaccharide density as a function of capsule radial distance. To study the polysaccharide density of the capsule, we first measured the volume released after different irradiation times by use of India ink and the amount of GXM (capture ELISA) or total polysaccharide (phenol sulfuric acid method) in the corresponding fractions. Significant amounts of GXM (Fig. 4A, gray bars) and total polysaccharide (data not shown) were released after each irradiation time. However, this amount released did not correlate with the amount of volume lost by the cells (Fig. 4A, solid line). The density of the various capsular regions was then calculated (Fig. 4B) from the amount of GXM released per cell (in μg), per volume (μl). The capsule GXM density was lowest at outer regions (~1.5 to 3 μm from the cell body) and dramatically increased at the inner regions (up to ~1.5 μm from the cell body). Interestingly, at the region closest to the cell wall, density decreased. This profile was also seen when total polysaccharide density was calculated (data not shown). The density profiles obtained from total polysaccharide and GXM measurements were similar, strongly suggesting that the total polysaccharide content in the capsule correlated with GXM concentration. These observations are consistent with data indicating that GXM is the major component of capsule mass. In addition, these results indicate that polysaccharide distribution varies as a function of radial distance in the capsule.

Structure of capsule layers observed by scanning electron microscopy. We examined gamma-irradiated cells by SEM to ascertain whether the measured differences in density correlated with the visual appearance of the cells. We observed that gamma irradiation exposed distinct regions of the capsule

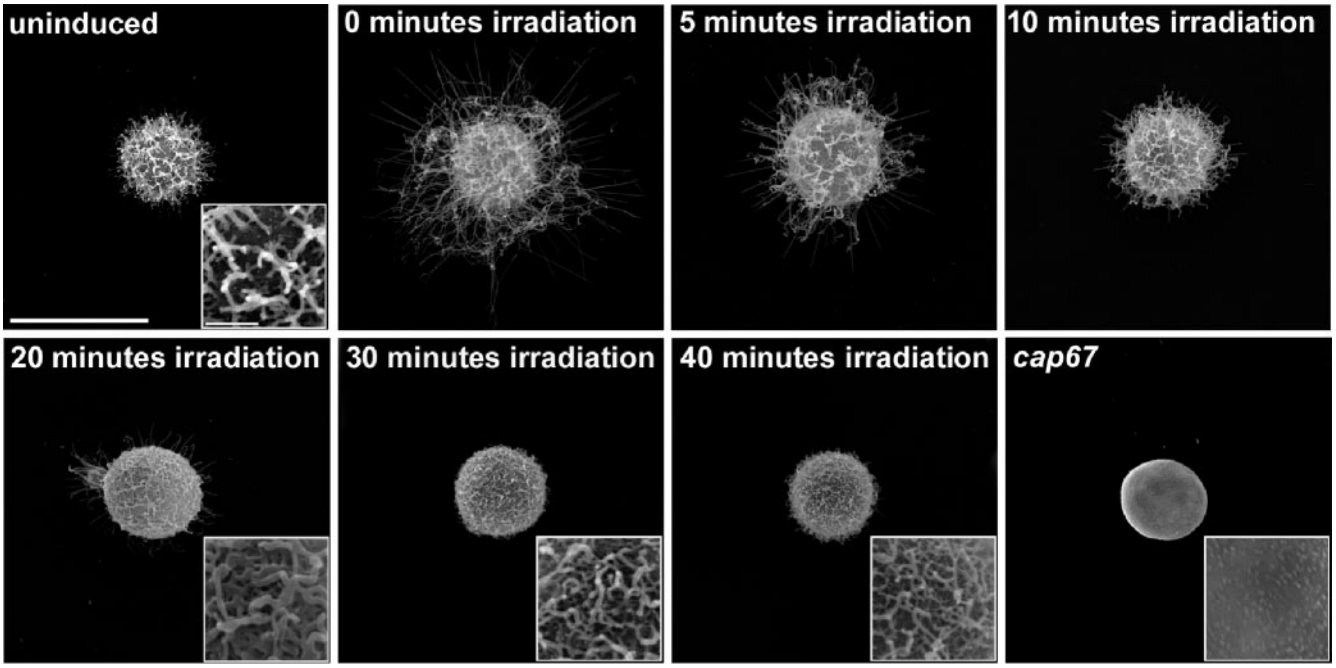

FIG. 5. Scanning electron microscopy of gamma radiation-exposed capsule regions. Yeast cells with induced capsule were irradiated for 0, 5, 10, 20, 30, and 40 min and then used to prepare samples for scanning electron microscopy. Bar, 5 μm (0.5 μm for inset). Scanning electron micrographs of cells in which the capsule was not induced (H99 grown in Sab) and of the acapsular *cap67* mutant served as controls.

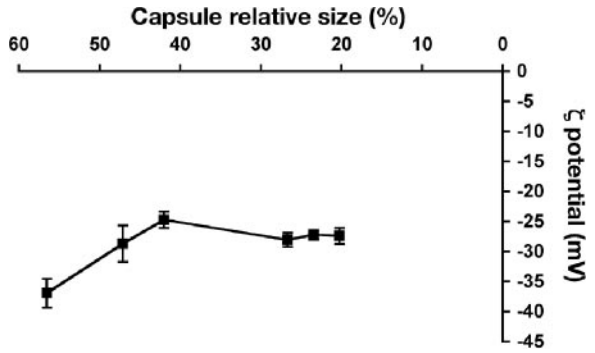

FIG. 6. Zeta potential of the capsule after gamma irradiation. After irradiation for 0, 5, 10, 20, 30, or 40 min, the zeta potential of the exposed capsule was measured and compared to capsule relative size, as determined by India ink staining. The average and standard deviation in a representative experiment are shown.

which differed in structural packing and organization (Fig. 5). Nonirradiated (untreated) cells appeared to be surrounded by two levels of organized polysaccharide (Fig. 5, time zero panel). The outer capsule seemed to be a diffuse web of fibers, while the inner capsule resembled a dense net. Irradiation for up to 20 min removed the outer layer but did not affect the visually dense region, which is consistent with the high-density region predicted by calculation (Fig. 4B). This tight network of polysaccharide around the cell body differed from the capsule organization observed for cells prior to capsule enlargement (uninduced). Comparisons to the *cap67* mutant, which lacks a capsule, confirmed that even after 40 min of irradiation, some capsular polysaccharide remained associated with the cell. These results are consistent with differential organization of polysaccharide fibers according to their radial location in the capsule, although assumptions on the nature of capsule structure based on electron microscopy must be made with caution. SEM sample preparation requires serial dehydration, which may affect final capsule structure. Regardless, the SEM data are consistent with the density calculations (Fig. 4B) and suggest that capsule enlargement is accompanied by a significant increase in the amount of polysaccharide in the capsule.

Charge distribution throughout the capsule. *C. neoformans* cells are highly negatively charged, due to the large amount of glucuronic acid present in the capsule. As a consequence, the zeta potential obtained for nonencapsulated *C. neoformans* strains and other fungi is much lower than that for encapsulated cryptococcal cells (48). Consequently, we measured the zeta potential of the cells after different doses of gamma irradiation (Fig. 6). Untreated cells had the lowest zeta potential, at −37 mV. Zeta potential increased as a function of decreasing capsule thickness, suggesting that the charge distribution is not equal throughout the capsule. In regions where the density was predicted to be higher, zeta potential did not significantly change.

Sugar composition and elemental analysis of the different polysaccharide fractions. To determine if the changes observed in polysaccharide density and charge were related to changes in the sugar composition of the capsular regions, the carbohydrate composition in the different polysaccharide fractions was analyzed. No significant differences were observed in the sugar compositions of the different fractions (data not shown), but subtle differences in the molar ratios may have been masked by the large volume of capsule released in the first 20 min of irradiation. Therefore, we prepared two different fractions of the capsule by irradiating cells for 20 min, collecting supernatants, washing cells in H_2O, and resuspending them in new medium for 20 min of further irradiation. We chose 0 to 20 min and 20 to 40 min, since the fractions obtained with these irradiation times corresponded to the low- and high-density regions of the capsule, respectively. However, no difference was detected in the sugar compositions of the different fractions (Table 1). The presence of galactose indicates that GalXM is also released in the corresponding fractions. In addition, the elemental compositions of the 0- to 20-min and 20- to 40-min fractions were analyzed for carbon, oxygen, nitrogen, and hydrogen (Table 2). There was no difference in the proportion of these elements, a finding which is in agreement with the results obtained from the sugar composition. The relative paucity of nitrogen is consistent with a capsular structure com-

TABLE 1. Glycosyl composition analysis of supernatants from gamma-irradiated cryptococcal cells

Glycosyl residue	Mol%[a] for irradiation period[b] (min)	
	0–20	20–40
Xylose	38.4	35.9
Glucuronic acid	10.1	7.4
Mannose	34.7	32.1
Galactose	5.6	4.5

[a] Values are expressed as moles percent of total carbohydrate. Results of a representative experiment are shown.
[b] Time of exposure of *C. neoformans* strain H99 to ^{137}Cs, which emits gamma radiation at the dose of 1,388 rads/min.

TABLE 2. Qualitative elemental analysis of supernatants from gamma-irradiated cryptococcal cells

Element	Wt %[a] for irradiation period (min)[b]	
	0–20	20–40
Carbon	40	40
Hydrogen	6	6
Nitrogen	0.7	0.5
Oxygen	45	44

[a] Values are expressed as weight percentage of each element analyzed.
[b] Time of exposure of *C. neoformans* strain H99 to ^{137}Cs, which emits gamma radiation at the dose of 1,388 rads/min.

TABLE 3. Scatchard analysis of H99 capsular regions exposed by gamma radiation[b]

Irradiation time (min)[a]	K_a (10^7, M^{-1})	No. of binding sites/cell (10^5)
None (untreated)	29.0	5.9
10	4.9	7.0
20	5	7.4
30	12.0	4.6
40	8.0	7.3

[a] Time of exposure of *C. neoformans* strain H99 to ^{137}Cs, which emits gamma radiation at the dose of 1,388 rads/min.
[b] Values were determined by Scatchard analysis as described in reference 32. The experiment was done in duplicate, with very similar results being obtained. Data from a representative experiment are shown.

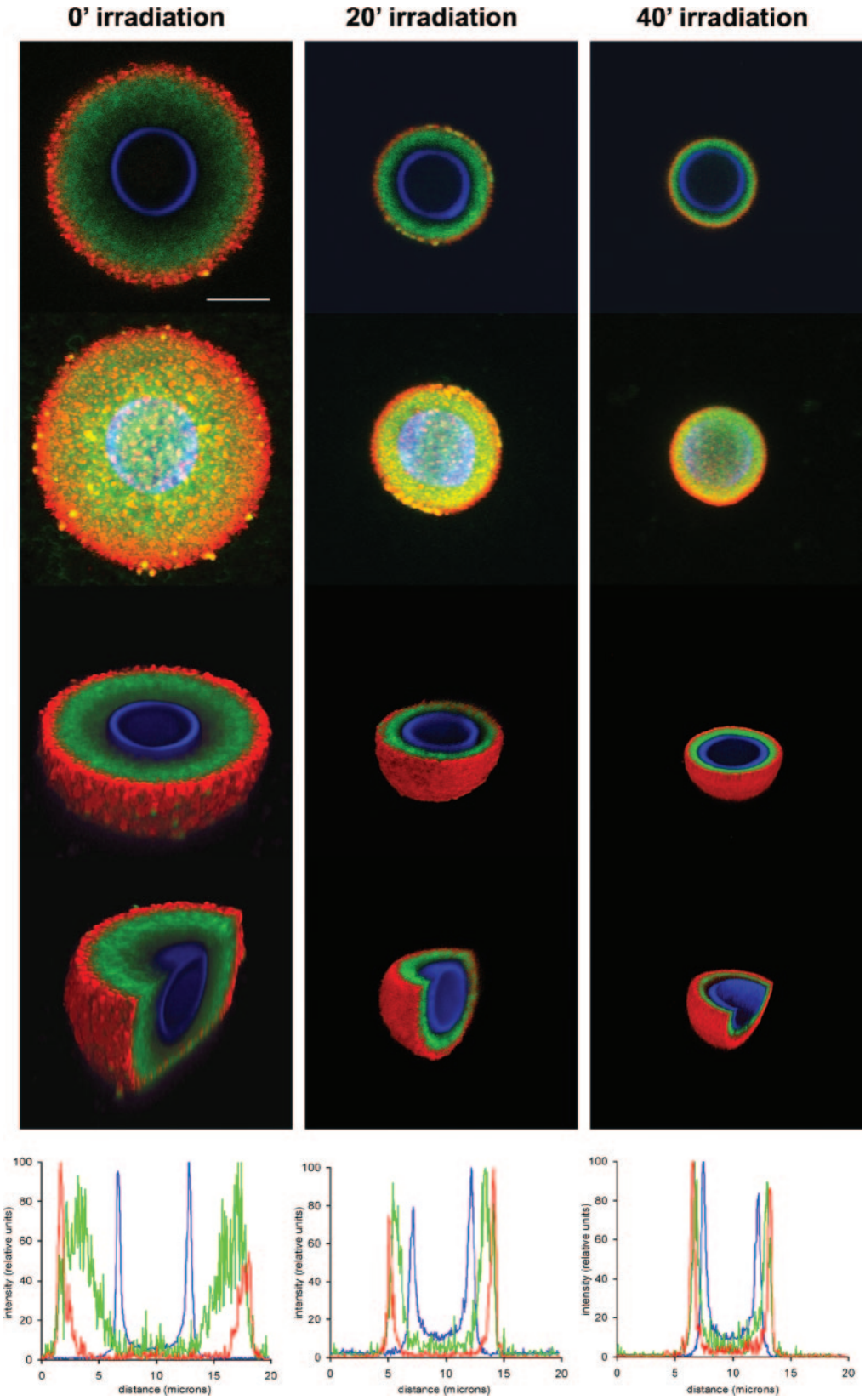

FIG. 7. 18B7 epitope distribution in the *C. neoformans* capsule. Cells were gamma irradiated for 0, 20, or 40 min and then labeled with 18B7-FITC. The cell wall was detected using calcofluor, and the capsular edge was detected by 12A1/goat anti-mouse IgM-TRITC. Pictures were taken using confocal microscopy. Panels show, for each period of gamma radiation, merged immunofluorescence labels, 3D reconstruction (ImageJ software), 3D *z* slice (Voxx software), 3D *z/y* slice (Voxx), and fluorescent signal intensity profiles (ImageJ) (top to bottom, respectively). Scale bar, 5 microns.

posed almost entirely of polysaccharide with little or no protein. Concerning the sugar analysis, this was performed on supernatants from cells irradiated for 5, 10, 20, 30, and 40 min (without washes), and the results were the same (data not shown). The proportion of the elements measured is similar to the values obtained with purified GXM (D. C. McFadden, personal communication), which confirms that most of the mass obtained from the capsule is GXM.

Antigenic properties of the different regions of the capsule. Given the apparent mass density and charge differences in the capsular layers, we evaluated changes in the antigenic structure of the *C. neoformans* capsule after graded exposure to gamma radiation. Previous studies used Scatchard analysis to calculate the number of binding sites and the binding affinity (K_a) of the ^{188}Re-labeled MAb 18B7 for the capsule after enlargement (15). We performed Scatchard analysis using ^{188}Re-labeled 18B7 for cells irradiated for 0, 10, 20, 30, and 40 min) (Table 3). Surprisingly, the number of binding sites and K_a showed that while the number of binding sites was equal throughout the capsule, the affinity of the antibody for the binding sites dramatically changed. The higher-affinity binding sites for 18B7 were located at the outer and inner capsular regions (regions 1, 4, and 5). The central regions of the capsule (regions 2 and 3) had lower-affinity binding sites.

The number of binding sites in the capsule remains relatively constant regardless of the irradiation time. In contrast, the mass density, charge, and affinity of MAb 18B7 changed as a function of capsule radial distance. Therefore, we chose to evaluate whether the constant of number of binding sites represented an average of 18B7 binding throughout the capsule, skewed by binding at high-affinity inner sites. When 18B7 binding was visualized by immunofluorescence using secondary antibodies, an annular binding pattern (70) was seen at the perimeter of the capsule and scanning electron micrographs showed a similar MAb cross-linking the capsule surface (13). To investigate if this was a consequence of the secondary MAb failing to penetrate the capsule surface and to compare the results obtained from the Scatchard analysis, we visualized the distribution of 18B7 within the capsule, by using MAb 18B7 directly conjugated to FITC and confocal microscopy. The cell wall of *C. neoformans* was labeled with calcofluor, and an IgM antibody to GXM (12A1) was used to visualize the capsule edge. The fluorescence of each label was analyzed by confocal microsopy, and signal intensity was plotted per μm of distance (Fig. 7).

MAb 18B7 was distributed throughout the capsule, although a distinct gap of fluorescence was observed between the cell wall (calcofluor signal) and MAb 18B7. We also observed that there was a gap between the signal of 18B7 and the capsule edge, since the fluorescence of MAbs 18B7 and 12A1 did not colocalize at the capsule edge. The same results were obtained when we used MAb 18B7 conjugated to TRITC or when we detected capsule edge using MAb 13F1 (results not shown). Localization of MAb in the capsule by confocal microscopy was consistent with the idea that the number of binding sites seen from Scatchard analysis in nonirradiated cells and cells irradiated for 10 or 20 min includes binding sites in the inner capsule, although the binding sites exposed after 30 or 40 min most likely represent new epitopes that are not accessible initially by MAb 18B7 due to the high density of this region.

Cell age affects the susceptibility to gamma radiation. We observed that the amount of capsule released after gamma radiation was dependent on capsule age. In preliminary experiments, *C. neoformans* cells incubated for 7 or 14 days in capsule enlargement medium seemed to become resistant to gamma radiation (Fig. 8A). In these conditions, the size of the capsule did not significantly change after 1 day of incubation, as already reported (71). Capsule age could be an important factor when considering host infection and survival of the yeast in the environment. After cells were irradiated for 0, 20, or 40 min, the decrease in capsule size was measured (Fig. 8B). After 7 and 14 days of incubation, the capsule size of the population was heterogeneous; therefore, the average volume was measured using hematocrit tubes (36). This heterogeneity most likely results from the limited period of budding that occurs in capsule enlargement medium before nutrient exhaustion. The new buds generated do not have enough nutrients to build a capsule or grow in size. Nonetheless, when the decrease in capsule volume was measured as a percentage of the original capsule for cells induced overnight and cells with capsule induced after 7 and 14 days, the cells with capsule induced after 7 and 14 days were increasingly more resistant to gamma radiation. This suggests that over time, changes occurred in the enlarged capsule of *C. neoformans*, which may be due to changes in the capsular structure and cross-linking of GXM fibers.

A method to distinguish budded progeny from cells inoculated into the capsule-inducing medium was developed to enable a more precise analysis of the effect of capsule age on gamma radiation sensitivity. Cryptococcal cell wall was labeled with sulfo-NHS-LC-biotin prior to inoculation into capsule induction medium. The biotin covalently binds to the cell wall and does not segregate to the bud. In this way, the original inoculum of cells after incubation with TRITC-conjugated streptavidin and immunofluorescence was identified. After biotin labeling, cells were incubated overnight or for 7 days in capsule-inducing medium and irradiated for 0, 20, or 40 min. The capsule edge was visualized with MAb 18B7 and detected by secondary antibody. Capsule size was measured on biotin-positive cells (Fig. 9A). After 7 days of incubation in inducing medium, biotin-positive cells had a larger capsule size after gamma irradiation than did cells incubated overnight, measured by capsule volume percent decrease (Fig. 9B) or by comparison of changes in capsule relative size (Fig. 9C). The percent capsule decrease calculated here reproduced the values calculated using hematocrit volume measurements of the heterogeneous population (Fig. 8B).

Finally, to get insight into whether there were structural differences between young and old induced capsule, we performed scanning electron microscopy on cells incubated in capsule-inducing medium for 7 days and irradiated for 0, 20, or 40 min (Fig. 10 compared to Fig. 5). We observed the accumulation of a high density of polysaccharide fibers in a significant portion of the population throughout the capsule, compared to cells induced overnight (Fig. 10 and 5). In addition, it was obvious that fibers on gamma-irradiated cells were longer than those observed on cells induced overnight. This is another indication of gamma radiation resistance in older capsule cells.

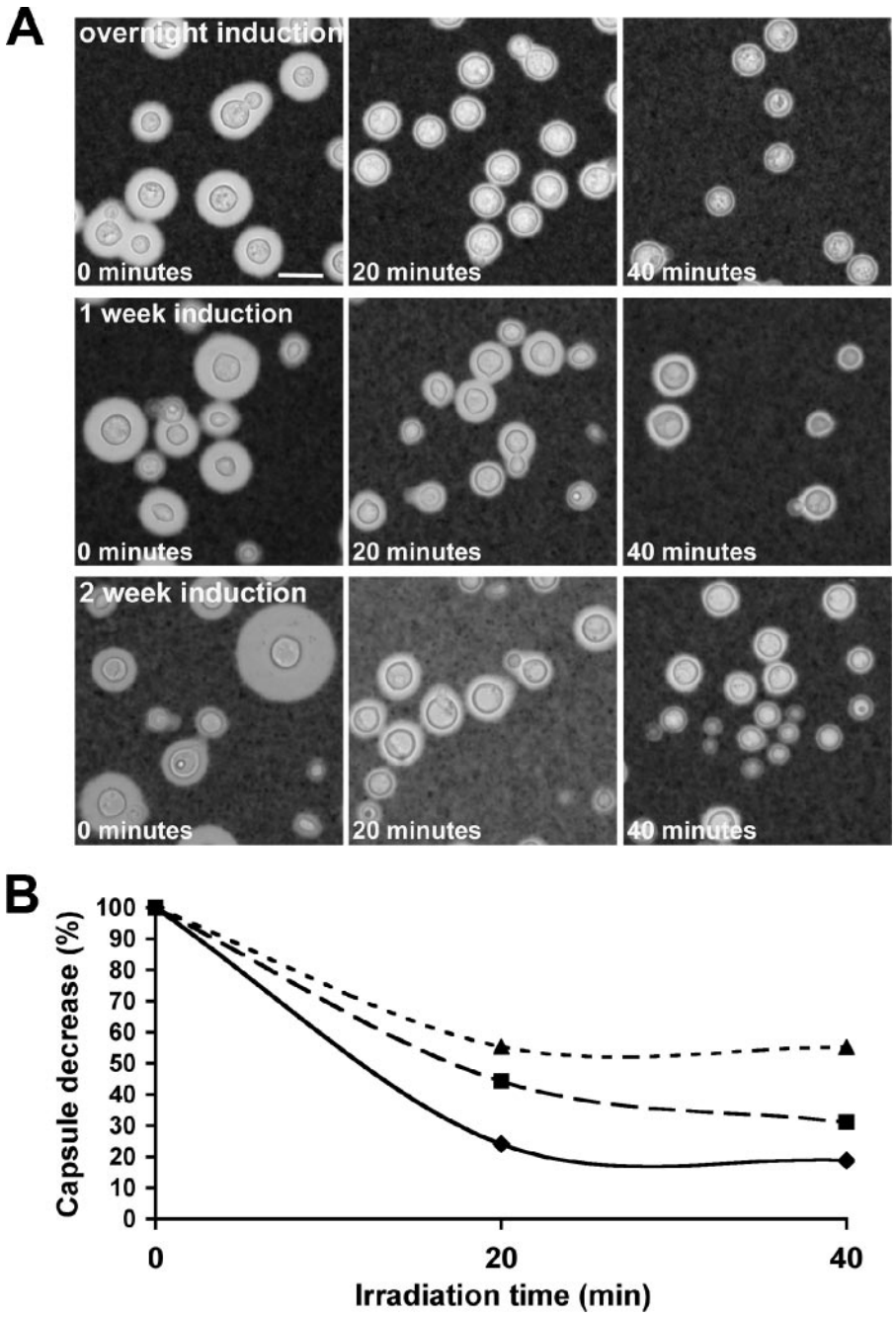

FIG. 8. Effect of capsule age on capsule sensitivity to gamma irradiation. (A) After incubation of cryptococcal cells in capsule-inducing conditions overnight or for 7 or 14 days, cells were gamma irradiated for 0, 20, or 40 min, and the population was observed by India ink staining. (B) Decrease in capsule size of cells, based on hematocrit cell packing, as a result of gamma irradiation for overnight (◆), 7-day (■), or 14-day (▲) cultures. The calculations were based on the percent volume of the 0-min (untreated) sample. Average capsule volumes were measured by hematocrit cell packing.

DISCUSSION

Gamma irradiation causes radiolysis of water, resulting in short-lived free radicals that can react with polysaccharides and break glycosyl linkages (44, 57). Therefore, it is likely that capsule release following gamma irradiation occurs as a result of free radical attack on the capsule (6). Several lines of evidence discussed below suggest that this free radical attack occurs only on the outer surface. Cryptococcal cells labeled at the inner capsule by C3 did not show any changes in the organization of this region, as manifested by changes in the radial position of the C3 label. Although previous work had shown that gamma radiation exposure resulted in release of the C3 binding region of the capsule (71), those studies involved cells with small, noninduced capsules where gamma radiation resulted in almost total release of the polysaccharide. For cells with large induced capsule, C3 binds to the innermost

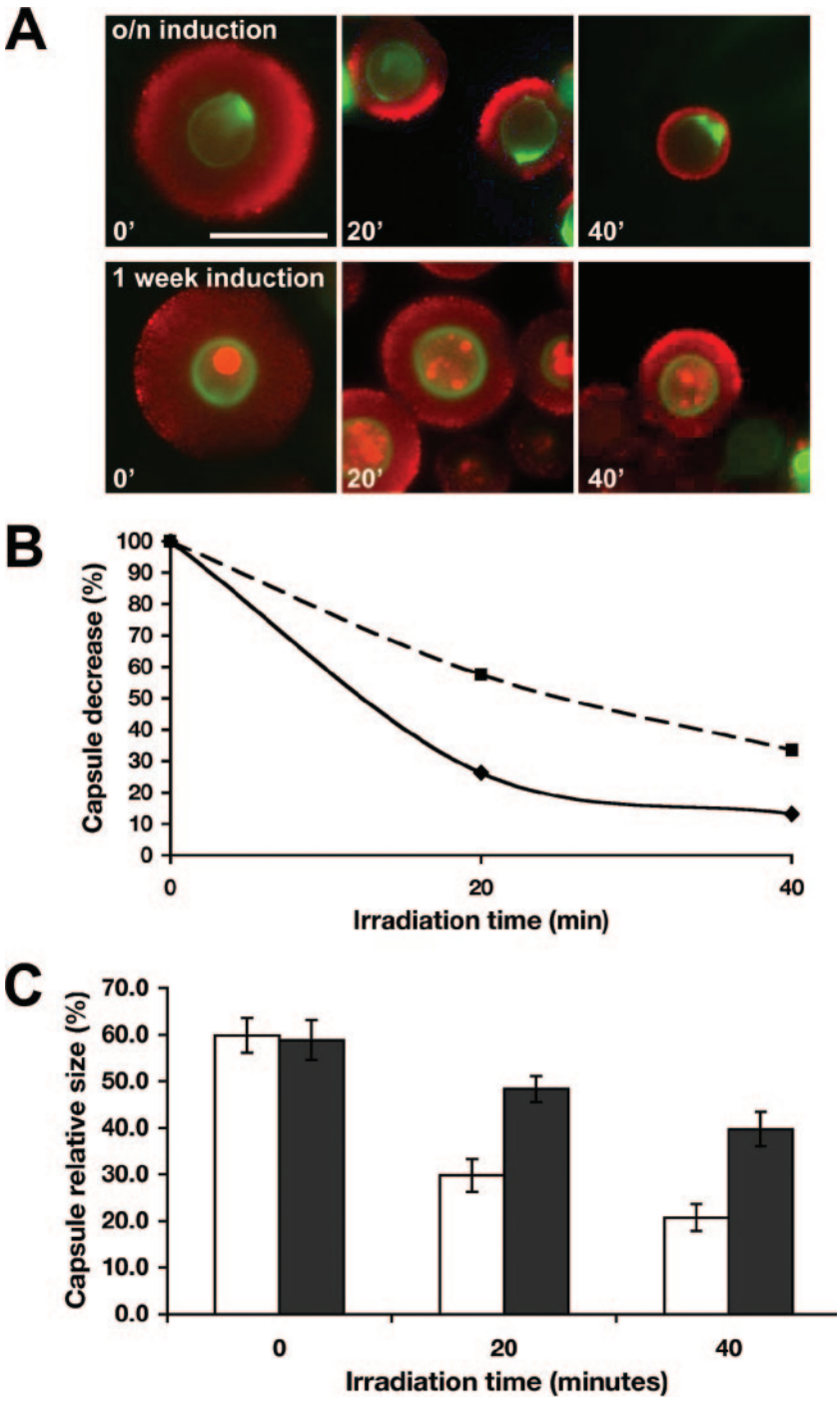

FIG. 9. Biotin labeling of *C. neoformans* cells to identify older cells and quantify gamma radiation resistance. (A) Prior to induction, cells were labeled with EZ-Link sulfo-NHS-LC-biotin. After incubation overnight or for 7 days in capsule-inducing conditions, cells were gamma irradiated for 0 (untreated), 20, or 40 min, and the original inoculation was detected with streptavidin-FITC. The capsular edge was detected using 13F1 and goat anti-mouse IgM-TRITC. Bar, 10 μm. (B) Decrease in capsule size of cells as a result of gamma irradiation, for overnight (■) and 7-day (◆) cultures. The calculations were based on the percent volume of the 0-min (untreated) sample. The average capsule volumes were measured for biotin-positive cells. (C) Capsule relative size from at least 20 cells, for overnight (open bars) or 7-day (closed bars) cultures, which were then irradiated for different periods of time. Capsule relative size was measured for biotin-positive cells by immunofluorescence.

layer, which is not released by gamma radiation. In a supporting experiment, we observed that coating of the capsule with MAb 18B7 conferred protection against gamma radiation on the capsule at high antibody concentration, while at lower concentrations the MAb was removed from the outer capsule by gamma radiation-induced attack. Protection of the capsule from gamma radiation by antibody is consistent with the observation that antibody prevents polysaccharide shedding (35).

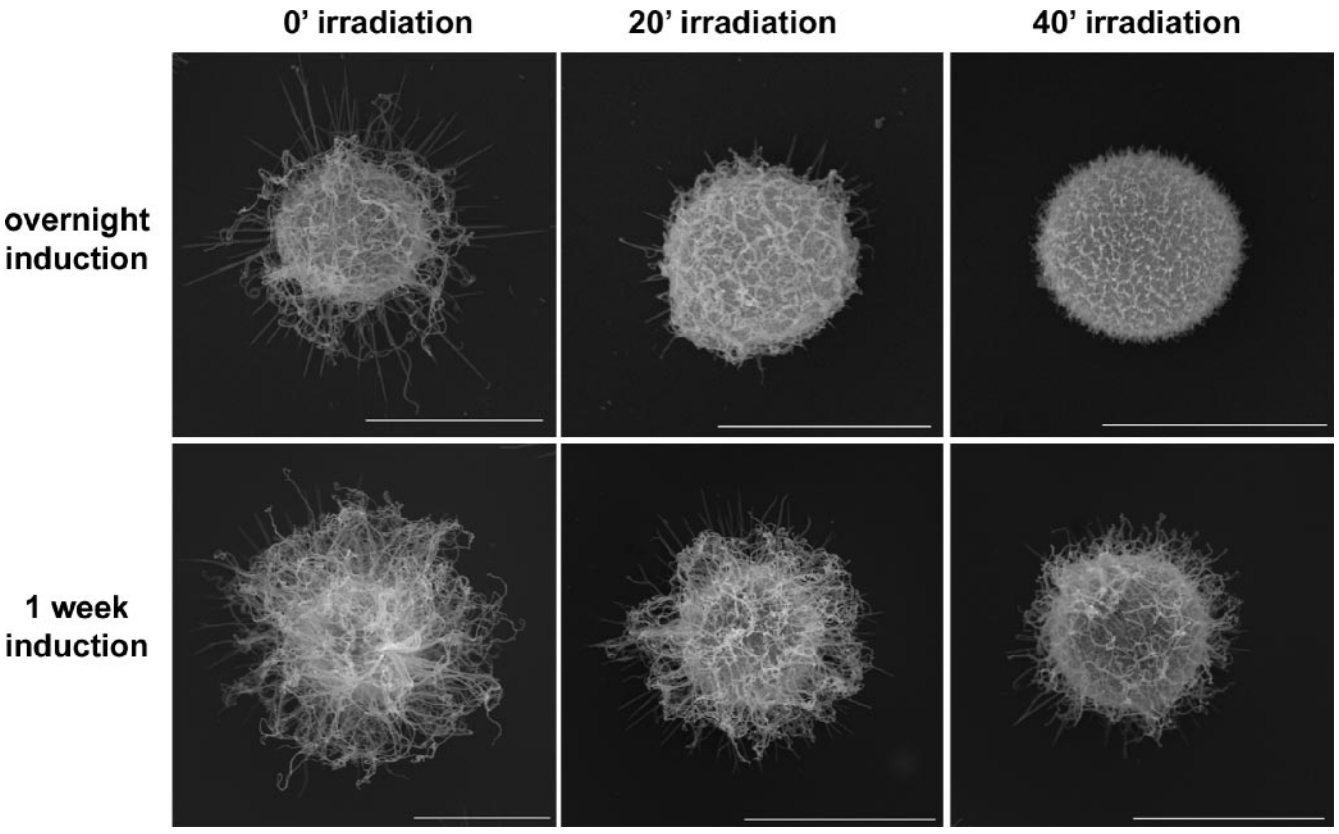

FIG. 10. SEM comparison of young and old cells exposed to gamma radiation. *C. neoformans* cells were incubated overnight (upper row) or for 7 days (lower row) in capsule-inducing conditions. Cryptococcal cells were then gamma irradiated for 0, 20, or 40 min and imaged by scanning electron microscopy. Bars, 5 μm.

In antibody-coated cells, the immunoglobulin could quench free radicals produced by gamma radiation and reduce polysaccharide release by protecting the GXM. In this regard, the observation that antibody binding blocks the capsule release induced by free radicals could be an important consideration when studying the immunoregulatory effects of extracellular GXM during host infection. Overall, our results imply that the products of radiolysis formed after gamma radiation treatment react preferentially with capsule surface polysaccharides.

Capsule density varies dramatically at different regions of the capsule, with a trend toward decreasing density as distance from the cell increases. Previous reports support these changes in density in the capsule (23, 50), although one account was based on MAb (Fab fragments) accumulation in the capsule (23), where it is possible that the penetration of the MAb into the inner regions was compromised. Our results give direct quantitative measurement of the polysaccharide distribution. When we compared capsule density with the results previously described in the literature, we found consistent results (23), although our density values are higher than that reported. We think this difference is due to the experimental approach, since our conditions (measurement of released GXM) presumably detect epitopes in GXM that are not accessible when the polysaccharide fibers are entangled within the capsule. The fact that independent experimental approaches gave consistent results confirms that capsule density varies as a function of the radial density. Interestingly, the density of the capsule peaked at about 1 μm from the cell and subsequently decreased at the innermost region, in agreement with micrograph images obtained after high-pressure freezing of the capsule (50). Although not understood, it is possible that this inner region is strongly attached to the cell wall and plays an important role in stabilizing the capsule and providing a structural framework for the addition of new fibers in the higher-density region. These changes in polysaccharide density after capsule enlargement support the current model of capsule growth, in which the newer fibers of polysaccharide intercalate between the existing ones, enlarging the capsule distally (40, 71). This model supports our observations because it predicts an increase in density proximal to the cell wall, where this intercalation would occur, and a decrease in density distal to the cell wall, where extension occurs. In addition, the higher density in the inner capsule offers an explanation for its increased resistance to gamma radiation. Our results are consistent with previous findings that revealed that the inner part of the capsule was more resistant to release by dimethyl sulfoxide (DMSO) (23) or gamma radiation (6). This density distribution suggests a protective role during the interaction with the host, since it could prevent the penetration of molecules such as defensins and antibodies into the cell, on the basis of molecular size (23). Moreover, recent findings indicate that India ink atypically penetrating into the capsule does not permeate the inner high-density regions of the capsule, instead forming an equatorial ring-like structure at the midcapsule (69).

By exposing different regions of the capsule structure, differences in physical and antigenic properties were demonstrated. We observed changes in the zeta potential of the cells, decreasing as the radius of the capsule increased. This is in agreement with previous findings that showed a similar correlation between the zeta potential and capsule volume of different cryptococcal strains with various capsule sizes (48). We do not have a clear explanation for this result. The slight difference in the glucuronic proportion could be partially responsible for this effect. Zeta potential is the electrostatic potential of the area that surrounds the particle that is measured (54) and does not directly reflect the charge of the particle. The measured zeta potential is proportional to the charge of the particle, dependent on the dielectric constant and viscosity of the medium and on the mobility of the particle. Since the medium remained the same between samples, the difference in the zeta potential in the irradiated cells suggests dissimilarities in the exposed capsule regions that affect the characteristics of the surface around the cells. Changes in zeta potential may have significance in host interactions, since they have been proposed/shown to affect the outcome of phagocytosis (1, 59).

We also studied the antigenic properties of the different regions of the capsule by Scatchard analysis of MAb 18B7 binding to GXM. Our observations suggest that there is a great immunogenic variance within the capsule and that there are high- and low-affinity binding sites present. To further understand the localization of this antibody, we analyzed the distribution of fluorescently conjugated MAb 18B7 by confocal microscopy and showed that in fact this MAb localizes to the middle-outer regions of the capsule but not to the region closest to the cell wall. The antibody is most likely unable to reach the epitopes at inner regions due to the increased density of the fibers, since these inner epitopes became available for antibody binding only after 30 and 40 min of irradiation. Furthermore, antibody cross-linking of fibrils in the outer layers of the capsule may reduce penetration of subsequent molecules (67). This implies that for cells irradiated for less than 30 min, where the high-density region of the capsule was unexposed, the determined number of binding sites is actually a measure of the binding sites in the entire low-density capsule region. Intuitively, the actual number of binding sites per capsular region would be only a fraction of the total binding sites. This more closely correlates with the density trend. The localization of MAb 18B7 to the inner capsule, where there are epitopes with moderately high affinity, could represent a mechanism for immune evasion, since circulating antibodies would have to compete for binding at the capsule edge and interior. Binding at the latter location would render the antibody unavailable for Fc receptor binding on phagocytic and antigen-presenting cells. All this together suggests that the difference in epitope distribution in the polysaccharide capsule could represent a relevant mechanism for the interaction between the pathogen and the host.

In addition to the differences in epitope distribution or organization, we found no significant differences in C, H, and O proportions or in the sugar composition throughout the capsule. We found a trend toward decreasing glucuronic acid in regions closer to the cell wall. Previous reports (6) have described a difference in glucuronic acid, with this sugar being present in significantly lower concentrations in the inner regions of the capsule. Although our results might appear to be in discrepancy, the previous report used a combination of DMSO and gamma radiation to release the capsule, a treatment that also removes the inner part of the capsule, a region that remains attached to the cell in our conditions. In addition, DMSO can affect intracellular membranes and release some intracellular polysaccharides, which could further alter the measured sugar composition.

Finally, we have established that the susceptibility of cells to gamma radiation decreases with capsule age. Our findings suggest that capsule age is associated with important changes in capsular structure, either in cross-linking and/or in the amount of polysaccharide present in the structure. This is a very significant finding, as the concept of capsule age is an important factor during host infection. Previous reports show that after incubation in capsule-inducing medium, the capsule grows in size but reaches a limit that correlates with cell size (71). The observations presented here indicate that with age, the capsule no longer grows in size but becomes denser by accumulation of polysaccharide, as suggested by the SEM images. This implies that during in vivo infection, where the fungal cells may stay in the lung for long periods of time, there are two major changes that occur in the capsule: first, enlargement in size (early response), which occurs during the first hours of infection (21), and second, increase in density and cross-linking (late response), which would require several days. The first response would prevent phagocytosis of the fungal cells by phagocytic cells present in the lung (29, 30, 43, 70). The second mechanism would protect the fungal cells against the immune defense mechanisms found in the granulomas, such as free radicals, which could damage the fungal cell. Our results have important implications during the last stage, since increasing the amount of polysaccharide in the capsule could protect the cell against a large number of molecules, such as free radicals, defensins, or antibodies, or by blocking penetration. In addition, it is known that the capsule suffers rearrangements in vivo to allow for adaptation to different organs and crossing of the blood-brain barrier (11, 22). Furthermore, it has been reported that prolonged incubation of *C. neoformans* in serum reduces the reactivity of its capsular polysaccharide to MAbs (42), indicating that the capsule may undergo rearrangements in vivo that allow for evasion of the host immune response, in this case, by avoiding Ab binding.

The results of this study present a detailed view of several undefined aspects of the cryptococcal capsule, the main virulence factor of this fungal pathogen. This structure is heterogeneous and complex in its radial organization, and this complexity increases with capsule age, as factors determining the amount and cross-linking of the polysaccharide fibers manifest. This complex organization provides insight into the protective role of the capsule during interactions of *C. neoformans* with the host.

ACKNOWLEDGMENTS

We are thankful to the Analytical Imaging Facility at Albert Einstein College of Medicine, especially to Michael Cammer, Rosana Leonard, Leslie Gunther, Clemenia Cayetano, and Juan Jiménez for their great help in the preparation, observation, and analysis of scanning electron micrographs and confocal images and with 3D image reconstruction. We warmly thank Diane McFadden for communication of unpublished results, helpful discussions, and critical reading of the manuscript. We thank Bettina Fries and Emily Cook for useful technical suggestions.

We thank Magdia De Jesus and Marcela Torres for the kind gift of the fluorescently labeled MAb 18B7 and Ekaterina Revskaya for help with Scatchard measurements.

Arturo Casadevall is supported by the following grants: AI33774-11, HL59842-07, AI33142-11, AI52733-02, and GM 07142-01. Ekaterina Dadachova is supported by grant AI60507. The glycosyl analysis was supported in part by the Department of Energy-funded (DE-FG09-93ER-20097) Center for Plant and Microbial Complex Carbohydrates.

REFERENCES

1. **Abbracchio, M. P., J. D. Heck, and M. Costa.** 1982. The phagocytosis and transforming activity of crystalline metal sulfide particles are related to their negative surface charge. Carcinogenesis **3:**175–180.
2. **Bacon, B. E., and R. Cherniak.** 1995. Structure of the O-deacetylated glucuronoxylomannan from *Cryptococcus neoformans* serotype C as determined by 2D 1H NMR spectroscopy. Carbohydr. Res. **276:**365–386.
3. **Bacon, B. E., R. Cherniak, K. J. Kwon-Chung, and E. S. Jacobson.** 1996. Structure of the O-deacetylated glucuronoxylomannan from *Cryptococcus neoformans* Cap70 as determined by 2D NMR spectroscopy. Carbohydr. Res. **283:**95–110.
4. **Bergman, F.** 1965. Studies on capsule synthesis of *Cryptococcus neoformans*. Sabouraudia **4:**23–31.
5. **Bose, I., A. J. Reese, J. J. Ory, G. Janbon, and T. L. Doering.** 2003. A yeast under cover: the capsule of *Cryptococcus neoformans*. Eukaryot. Cell **2:**655–663.
6. **Bryan, R. A., O. Zaragoza, T. Zhang, G. Ortiz, A. Casadevall, and E. Dadachova.** 2005. Radiological studies reveal radial differences in the architecture of the polysaccharide capsule of *Cryptococcus neoformans*. Eukaryot. Cell **4:**465–475.
7. **Casadevall, A., J. Mukherjee, and M. D. Scharff.** 1992. Monoclonal antibody based ELISAs for cryptococcal polysaccharide. J. Immunol. Methods **154:** 27–35.
8. **Casadevall, A., and J. R. Perfect.** 1998. *Cryptococcus neoformans*. ASM Press, Washington, DC.
9. **Casadevall, A., J. N. Steenbergen, and J. D. Nosanchuk.** 2003. 'Ready made' virulence and 'dual use' virulence factors in pathogenic environmental fungi—the *Cryptococcus neoformans* paradigm. Curr. Opin. Microbiol. **6:**332–337.
10. **Chang, Y. C., and K. J. Kwon-Chung.** 1994. Complementation of a capsule-deficient mutation of *Cryptococcus neoformans* restores its virulence. Mol. Cell. Biol. **14:**4912–4919.
11. **Charlier, C., F. Chretien, M. Baudrimont, E. Mordelet, O. Lortholary, and F. Dromer.** 2005. Capsule structure changes associated with *Cryptococcus neoformans* crossing of the blood-brain barrier. Am. J. Pathol. **166:**421–432.
12. **Cherniak, R., and J. B. Sundstrom.** 1994. Polysaccharide antigens of the capsule of *Cryptococcus neoformans*. Infect. Immun. **62:**1507–1512.
13. **Cleare, W., and A. Casadevall.** 1999. Scanning electron microscopy of encapsulated and non-encapsulated *Cryptococcus neoformans* and the effect of glucose on capsular polysaccharide release. Med. Mycol. **37:**235–243.
14. **Cruickshank, J. G., R. Cavill, and M. Jelbert.** 1973. *Cryptococcus neoformans* of unusual morphology. Appl. Microbiol. **25:**309–312.
15. **Dadachova, E., R. A. Bryan, C. Apostolidis, A. Morgenstern, T. Zhang, T. Moadel, M. Torres, X. Huang, E. Revskaya, and A. Casadevall.** 2006. Interaction of radiolabeled antibodies with fungal cells and components of immune system in vitro and during radioimmunotherapy of experimental fungal infection. J. Infect. Dis. **193:**1427–1436.
16. **Dembitzer, H. M., I. Buza, and F. Reiss.** 1972. Biological and electron microscopic changes in gamma radiated *Cryptococcus neoformans*. Mycopathol. Mycol. Appl. **47:**307–315.
17. **Doering, T. L.** 2000. How does *Cryptococcus* get its coat? Trends Microbiol. **8:**547–553.
18. **Dong, Z. M., and J. W. Murphy.** 1995. Effects of the two varieties of *Cryptococcus neoformans* cells and culture filtrate antigens on neutrophil locomotion. Infect. Immun. **63:**2632–2644.
19. **D'Souza, C. A., J. A. Alspaugh, C. Yue, T. Harashima, G. M. Cox, J. R. Perfect, and J. Heitman.** 2001. Cyclic AMP-dependent protein kinase controls virulence of the fungal pathogen *Cryptococcus neoformans*. Mol. Cell. Biol. **21:**3179–3191.
20. **Dubois, M., K. Gilles, J. K. Hamilton, P. A. Rebers, and F. Smith.** 1951. A colorimetric method for the determination of sugars. Nature **168:**167.
21. **Feldmesser, M., Y. Kress, and A. Casadevall.** 2001. Dynamic changes in the morphology of *Cryptococcus neoformans* during murine pulmonary infection. Microbiology **147:**2355–2365.
22. **Garcia-Hermoso, D., F. Dromer, and G. Janbon.** 2004. *Cryptococcus neoformans* capsule structure evolution in vitro and during murine infection. Infect. Immun. **72:**3359–3365.
23. **Gates, M. A., P. Thorkildson, and T. R. Kozel.** 2004. Molecular architecture of the *Cryptococcus neoformans* capsule. Mol. Microbiol. **52:**13–24.
24. **Goldman, D. L., S. C. Lee, and A. Casadevall.** 1995. Tissue localization of *Cryptococcus neoformans* glucuronoxylomannan in the presence and absence of specific antibody. Infect. Immun. **63:**3448–3453.
25. **Granger, D. L., J. R. Perfect, and D. T. Durack.** 1985. Virulence of *Cryptococcus neoformans*. Regulation of capsule synthesis by carbon dioxide. J. Clin. Investig. **76:**508–516.
26. **Kozel, T. R., and E. C. Gotschlich.** 1982. The capsule of *Cryptococcus neoformans* passively inhibits phagocytosis of the yeast by macrophages. J. Immunol. **129:**1675–1680.
27. **Kozel, T. R., W. F. Gulley, and J. Cazin, Jr.** 1977. Immune response to *Cryptococcus neoformans* soluble polysaccharide: immunological unresponsiveness. Infect. Immun. **18:**701–707.
28. **Kozel, T. R., S. M. Levitz, F. Dromer, M. A. Gates, P. Thorkildson, and G. Janbon.** 2003. Antigenic and biological characteristics of mutant strains of *Cryptococcus neoformans* lacking capsular O acetylation or xylosyl side chains. Infect. Immun. **71:**2868–2875.
29. **Kozel, T. R., G. S. Pfrommer, A. S. Guerlain, B. A. Highison, and G. J. Highison.** 1988. Strain variation in phagocytosis of *Cryptococcus neoformans*: dissociation of susceptibility to phagocytosis from activation and binding of opsonic fragments of C3. Infect. Immun. **56:**2794–2800.
30. **Kozel, T. R., A. Tabuni, B. J. Young, and S. M. Levitz.** 1996. Influence of opsonization conditions on C3 deposition and phagocyte binding of large- and small-capsule *Cryptococcus neoformans* cells. Infect. Immun. **64:**2336–2338.
31. **Kwon-Chung, K. J., and J. C. Rhodes.** 1986. Encapsulation and melanin formation as indicators of virulence in *Cryptococcus neoformans*. Infect. Immun. **51:**218–223.
32. **Lindmo, T., E. Boven, F. Cuttitta, J. Fedorko, and P. A. Bunn, Jr.** 1984. Determination of the immunoreactive fraction of radiolabeled monoclonal antibodies by linear extrapolation to binding at infinite antigen excess. J. Immunol. Methods **72:**77–89.
33. **Love, G. L., G. D. Boyd, and D. L. Greer.** 1985. Large *Cryptococcus neoformans* isolated from brain abscess. J. Clin. Microbiol. **22:**1068–1070.
34. **Macher, A. M., J. E. Bennett, J. E. Gadek, and M. M. Frank.** 1978. Complement depletion in cryptococcal sepsis. J. Immunol. **120:**1686–1690.
35. **Martinez, L. R., D. Moussai, and A. Casadevall.** 2004. Antibody to *Cryptococcus neoformans* glucuronoxylomannan inhibits the release of capsular antigen. Infect. Immun. **72:**3674–3679.
36. **Maxson, M. E., E. Cook, A. Casadevall, and O. Zaragoza.** 8 September 2006. The volume and hydration of the *Cryptococcus neoformans* polysaccharide capsule. Fungal Genet. Biol. [Epub ahead of print.] doi:10.1016/j.fgb.2006.07.010.
37. **McClelland, E. E., P. Bernhardt, and A. Casadevall.** 2006. Estimating the relative contributions of virulence factors for pathogenic microbes. Infect. Immun. **74:**1500–1504.
38. **McFadden, D. C., and A. Casadevall.** 2001. Capsule and melanin synthesis in *Cryptococcus neoformans*. Med. Mycol. **39**(Suppl. 1)**:**19–30.
39. **McFadden, D. C., and A. Casadevall.** 2004. Unexpected diversity in the fine specificity of monoclonal antibodies that use the same V region gene to glucuronoxylomannan of *Cryptococcus neoformans*. J. Immunol. **172:**3670–3677.
40. **McFadden, D. C., M. De Jesus, and A. Casadevall.** 2006. The physical properties of the capsular polysaccharides from *Cryptococcus neoformans* suggest features for capsule construction. J. Biol. Chem. **281:**1868–1875.
41. **McFadden, D. C., O. Zaragoza, and A. Casadevall.** 2006. The capsular dynamics of *Cryptococcus neoformans*. Trends Microbiol. **14:**497–505.
42. **McFadden, D. C., O. Zaragoza, and A. Casadevall.** 2004. Immunoreactivity of cryptococcal antigen is not stable under prolonged incubations in human serum. J. Clin. Microbiol. **42:**2786–2788.
43. **Mitchell, T. G., and L. Friedman.** 1972. In vitro phagocytosis and intracellular fate of variously encapsulated strains of *Cryptococcus neoformans*. Infect. Immun. **5:**491–498.
44. **Morelli, R., S. Russo-Volpe, N. Bruno, and R. Lo Scalzo.** 2003. Fenton-dependent damage to carbohydrates: free radicals scavenging activity of some simple sugars. J. Agric. Food. Chem. **51:**7418–7425.
45. **Moyrand, F., B. Klaproth, U. Himmelreich, F. Dromer, and G. Janbon.** 2002. Isolation and characterization of capsule structure mutant strains of *Cryptococcus neoformans*. Mol. Microbiol. **45:**837–849.
46. **Mukherjee, J., A. Casadevall, and M. D. Scharff.** 1993. Molecular characterization of the humoral responses to *Cryptococcus neoformans* infection and glucuronoxylomannan-tetanus toxoid conjugate immunization. J. Exp. Med. **177:**1105–1116.
47. **Murphy, J. W., and G. C. Cozad.** 1972. Immunological unresponsiveness induced by cryptococcal capsular polysaccharide assayed by the hemolytic plaque technique. Infect. Immun. **5:**896–901.
48. **Nosanchuk, J. D., and A. Casadevall.** 1997. Cellular charge of *Cryptococcus neoformans*: contributions from the capsular polysaccharide, melanin, and monoclonal antibody binding. Infect. Immun. **65:**1836–1841.
49. **Perfect, J. R., S. D. R. Lang, and D. T. Durack.** 1980. Chronic cryptococcal meningitis: a new experimental model in rabbits. Am. J. Pathol. **101:**177–194.
50. **Pierini, L. M., and T. L. Doering.** 2001. Spatial and temporal sequence of capsule construction in *Cryptococcus neoformans*. Mol. Microbiol. **41:**105–115.
51. **Reese, A. J., and T. L. Doering.** 2003. Cell wall alpha-1,3-glucan is required

to anchor the *Cryptococcus neoformans* capsule. Mol. Microbiol. **50:**1401–1409.
52. **Reiss, E., M. Huppert, and R. Cherniak.** 1985. Characterization of protein and mannan polysaccharide antigens of yeasts, moulds, and actinomycetes. Curr. Top. Med. Mycol. **1:**172–207.
53. **Retini, C., A. Vecchiarelli, C. Monari, F. Bistoni, and T. R. Kozel.** 1998. Encapsulation of *Cryptococcus neoformans* with glucuronoxylomannan inhibits the antigen-presenting capacity of monocytes. Infect. Immun. **66:**664–669.
54. **Richmond, D. V., and D. J. Fisher.** 1973. The electrophoretic mobility of micro-organisms. Adv. Microb. Physiol. **9:**1–29.
55. **Rivera, J., M. Feldmesser, M. Cammer, and A. Casadevall.** 1998. Organ-dependent variation of capsule thickness in *Cryptococcus neoformans* during experimental murine infection. Infect. Immun. **66:**5027–5030.
56. **Scatchard, G.** 1949. The attraction of proteins for small molecules and ions. Ann. N. Y. Acad. Sci. **51:**660–672.
57. **Sharpatyi, V. A.** 1999. Radiochemistry of polysaccharides. Radiat. Biol. Radioecol. **39:**156–161.
58. **Sheng, S., and R. Cherniak.** 1997. Structure of the ^{13}C-enriched O-deacetylated glucuronoxylomannan of *Cryptococcus neoformans* serotype A determined by NMR spectroscopy. Carbohydr. Res. **301:**33–40.
59. **Tabata, Y., and Y. Ikada.** 1988. Effect of the size and surface charge of polymer microspheres on their phagocytosis by macrophage. Biomaterials **9:**356–362.
60. **Turner, S. H., R. Cherniak, E. Reiss, and K. J. Kwon-Chung.** 1992. Structural variability in the glucuronoxylomannan of *Cryptococcus neoformans* serotype A isolates determined by ^{13}C NMR spectroscopy. Carbohydr. Res. **233:**205–218.
61. **Vartivarian, S. E., E. J. Anaissie, R. E. Cowart, H. A. Sprigg, M. J. Tingler, and E. S. Jacobson.** 1993. Regulation of cryptococcal capsular polysaccharide by iron. J. Infect. Dis. **167:**186–190.
62. **Vecchiarelli, A.** 2005. The cellular responses induced by the capsular polysaccharide of *Cryptococcus neoformans* differ depending on the presence or absence of specific protective antibodies. Curr. Mol. Med. **5:**413–420.
63. **Vecchiarelli, A., C. Retini, C. Monari, C. Tascini, F. Bistoni, and T. R. Kozel.** 1996. Purified capsular polysaccharide of *Cryptococcus neoformans* induces interleukin-10 secretion by human monocytes. Infect. Immun. **64:**2846–2849.
64. **Wilkinson, J. F.** 1958. The extracellular polysaccharides of bacteria. Bacteriol. Rev. **22:**46–73.
65. **York, W. S., A. G. Darvill, M. McNeil, T. T. Stevenson, and P. Albersheim.** 1986. Isolation and characterization of plant cell walls and cell wall components. Methods Enzymol. **118:**3–40.
66. **Zaragoza, O., and A. Casadevall.** 2004. Experimental modulation of capsule size in *Cryptococcus neoformans*. Biol. Proced. Online **6:**10–15.
67. **Zaragoza, O., and A. Casadevall.** 2006. Monoclonal antibodies can affect complement deposition on the capsule of the pathogenic fungus *Cryptococcus neoformans* by both classical pathway activation and steric hindrance. Cell. Microbiol. **8:**1862–1876.
68. **Zaragoza, O., B. C. Fries, and A. Casadevall.** 2003. Induction of capsule growth in *Cryptococcus neoformans* by mammalian serum and CO_2. Infect. Immun. **71:**6155–6164.
69. **Zaragoza, O., E. E. McClelland, A. Telzak, and A. Casadevall.** 2006. Equatorial ring-like channels in the *Cryptococcus neoformans* polysaccharide capsule. FEMS Yeast Res. **6:**662–666.
70. **Zaragoza, O., C. P. Taborda, and A. Casadevall.** 2003. The efficacy of complement-mediated phagocytosis of *Cryptococcus neoformans* is dependent on the location of C3 in the polysaccharide capsule and involves both direct and indirect C3-mediated interactions. Eur. J. Immnunol. **33:**1957–1967.
71. **Zaragoza, O., A. Telzak, R. A. Bryan, E. Dadachova, and A. Casadevall.** 2006. The polysaccharide capsule of the pathogenic fungus *Cryptococcus neoformans* enlarges by distal growth and is rearranged during budding. Mol. Microbiol. **59:**67–83.